

ICPES 2025

40th INTERNATIONAL CONFERENCE ON PRODUCTION ENGINEERING - SERBIA 2025



University of Nis

Faculty of Mechanical

Engineering

DOI: <u>10.46793/ICPES25.145W</u>

Society of Production Engineering

Nis, Serbia, 18 - 19th September 2025

HYDROGEN EMBRITTLEMENT OF RECYCLED PRESSURE VESSEL STEEL P460NL

Tobias Walder¹, Fabian BOBNER¹, Thomas STAUBMANN¹, Hamdi ELSAYED¹, Fernando WARCHOMICKA¹, Rudolf VALLANT¹, Sveto CVETKOVSKI²

Orcid: 0009-0007-4386-3091; Orcid: 0009-0003-2627-3752; Orcid: 0009-0002-8833-7638; Orcid: 0009-0004-4061-5533; Orcid: 0000-0002-4909-8657; Orcid: 0000-0002-2450-7119; Orcid: 0000-0002-5609-9201;

¹Graz University of Technology, Institut of Materials Science, Joining and Forming, Graz, Austria

²Ss. Cyril and Methodius University in Skopje (UKIM) Faculty of Technology and Metallurgy

*Corresponding author: rudolf.vallant@tugraz.at

Abstract: Hydrogen embrittlement (HE) presents a critical challenge to the structural integrity of pressure vessels, especially those manufactured from recycled steel. This study explores the susceptibility of recycled P460 NL1 pressure vessel steel to hydrogen induced degradation. A comprehensive approach is employed, combining Slow Strain Rate Testing (SSRT) under electrochemical hydrogen charging, metallographic analysis, and Thermal Desorption Spectroscopy (TDS), to investigate the influence of microstructural characteristics on mechanical performance and hydrogen uptake. Both base metal and welded specimens are examined to assess the effects of welding on hydrogen behavior. Additionally, detailed microstructural investigations are carried out to evaluate the role of non-metallic inclusions, specifically their number, size, and morphology in the embrittlement mechanisms of both recycled and conventionally produced steels. This study aims to elucidate the relationship between hydrogen absorption, inclusions, and microstructural features in recycled steels, which are increasingly utilized in sustainable engineering applications. The findings are expected to enhance the understanding of embrittlement mechanisms in recycled steels and support the development of effective mitigation strategies against hydrogen-related failures.

Key words: P460NL1, HE, Electrochemical hydrogen charging, SSRT, TDS

1. INTRODUCTION

From the point of The European Green Deal [1] steel producers face two issues, which are

 Increasing the recycling share to reduce CO₂ emissions, i.e. use up to 100% scrap
 [2] higher hydrogen load on steel infrastructure, like tubes or vessels for energy supply, i.e. transport and production of hydrogen (gas or liquid solutions) [3,4]

In difference to conventional steel making from ore (Blast furnace and Linz-Donawitz Oxygen converter / BOF) the recycled steel is produced from scrap, remelted in the Electric Arc Furnace (EAF), where also the metallurgical deoxidation is performed,

afterwards going directly to the continuous casting and the hot-rolling mill for producing sheets. By this recycling procedure the CO₂-emission is reduced from 2.3 t (BOF) to 0.7 t (EAF) per ton raw steel. [5]

A higher susceptibility for Hydrogen Embrittlement (HE) or more specific Hydrogen Assisted Cracking (HAC) due to the higher amount of Non-Metallic-Inclusions (NMI) of a Recycled Steel (RSt) in comparison to Conventional Steel (CSt) should be expectable. Here especially sulfide inclusions (MnS) are to be mentioned, as they form segregation sites for hydrogen and can induce cracks. [6,7]

The H- absorption depends on the microstructural features of the steel, such as grain size, grain boundaries, dislocations, interstitial lattice sites, defects etc., which also depends on the production processes. HAC refers to the loss of ductility in metals caused by hydrogen absorption into the crystal lattice. The diffusion and concentration of atomic

hydrogen around zones of high triaxiality promote local embrittlement mechanisms [8] Transport of hydrogen through the metal is determined by diffusion between interstitial lattice sites and trapping of hydrogen at microstructural sites such as grain boundaries, dislocations, carbides, inclusions and precipitate particles. [9]

2. EXPERIMENTAL

The investigated Recycled Steel (RSt) and the Conventional Steel (CSt) examined for comparison purposes, both specified as P460NL1, are weldable fine grain steel sheets of 12 mm thickness. According to manufacturer's data they fulfill the european standard EN 10028-3 with regards to chemical composition and mechanical properties. To note that the RSt has too high N-content and is normalized rolled and the CSt in contrast is normalised rolled and tempered - s. [10]

Table 1. Chemical composition and mechanical properties of Recycled Steel (RSt) vs. Conventional Steel (CSt) P460NL1 acc. to manufacturers data and compared to EN 10028-3 (Nb, Ti, V analysed by IMAT OES Spectrolab 2.3).

wt.%	С	Si	Mn	Р	s	AI_{total}	N	Cr	Cu	Ni	Мо	Nb	Ti	٧	EV1	CEV
RSt	0.16	0.25	1.22	0.016	0.005	0.055	0.08	0.07	0.3	0.25	0.1	0.038	0.003	0.059	0.100	0.427
CSt	0.17	0.43	1.57	0.011	0.001	0.031	0.011	0.04	0.17	0.49	0.01	0.03	0.003	0.09	0.123	0.504
EN 10028-3	<u>≤</u> 0.20	<u>≤</u> 0.60	1.10-1.70	<u>≤</u> 0.025	≤0.008	<u>≥</u> 0.020	<u><</u> 0.025	<u>≤</u> 0.30	<u>≤</u> 0.30	<u><</u> 0.80	<u><</u> 0.10	<u>≤</u> 0.05	<0.03	<u><</u> 0.20	<u><</u> 0.22	<u>≤</u> 0.53
								E	V1: V+T	ï+Nb	CE\	/ = C + I	Mn/6 + (Cr+Mo+	V)/5 + (N	i+Cu/15)

	R _{eH} (MPa)	R _m (MPa)	A ₅ %	ISO-V(-20) J 2)
RSt	512	627	29	144 (-20°C)
CSt 1)	537	639	24	119 (-50°C)
EN 10028-3	<u>≥</u> 460	570-730	<u>≥</u> 16	≥35 (-20°C)
		1	normalised & tempere	d ²⁾ transverse

The electrochemical H-charging without mechanical load was performed on 4-edged samples 5x5x24mm³ from the 12mm sheets for 1, 4, 8, 12 and 24 hours at approx. -3mA/cm² cathodic current density in a 3.5% NaCl solution at room temperature, adding 1g/l thiourea as a H-recombination poison. Afterwards the samples were cooled in liquid nitrogen and the TDA measurements performed.

The electrochemical H-charging with mechanical load was performed on tensile samples A5 x 25 acc. to standard DIN 50125, cutted out in the sheets rolling direction for Slow Strain Rate Tests (SSRT) acc. to ASTM G129-21 with a strain rate of 10⁻⁵/s. The SSRT were performed in air and with electrochemical H-charging conditions as explained above.

Submerged Arc Welding (SAW) without preheating was performed on the RSt and subsequently A5 x 25 tensile specimens manufactured, which include the weld and investigated in SSRT as explained above. The welding parameters are shown in Table 2.

Table 2. Welding parameters of Tandem SAW procedure of the RSt on 12mm sheet without preheating - V-joint outer and inner pass.

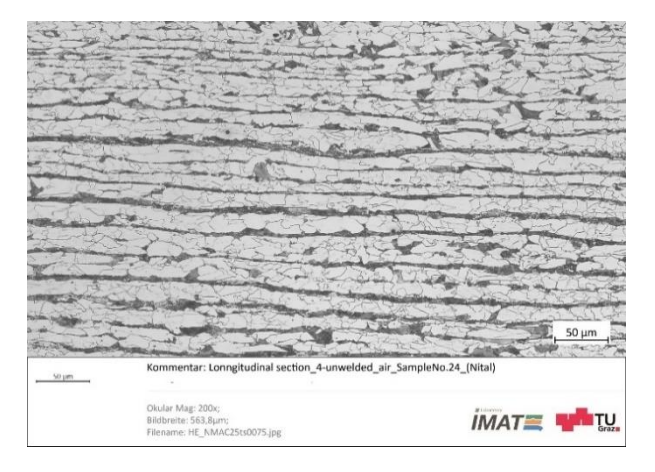
Welding	Welding	1 st pass - outer pass	Heat Input,	
wire	flux	2 nd pass - inner pass	kJ/cm	
EMS 2 Mo,	BB 24	Wire 1: 630 A, 30V, 1m/min	24 kJ/cm	
Ø 4 mm		Wire 2: 650 A, 33V, 1m/min	(11 + 13)	

After the SSRT fracture pieces were cooled in liquid nitrogen and subsequently the H-uptake determined in a Thermal Desorption Analysis (TDA) device *Bruker Galileio G8* with a detection limit (DL) of 0.01 wppm.

3. RESULTS

Microstructure of base materials, weld and inclusion analyses

In Light Optical Microscope (LOM) the Nital etched longitudinal section of the RSt show banded structures of Ferrite (77%) and Pearlite (23%). The width of the bands is approx. 10 µm for the Pearlite and 30 µm for the Ferrite. In contrast the CSt is in tempered condition and show finer and less pronounced banded structure, whereby the Pearlite bands are partially dissolved in forming carbides. The microstructure of the SAW weld, performed just on the RSt, consists mainly of Acicular Ferrite (AF), Bainite (B) and Grain Boundary Ferrite (GBF) and is thus completely different to the RSt base material microstructure - s. Figure 1.





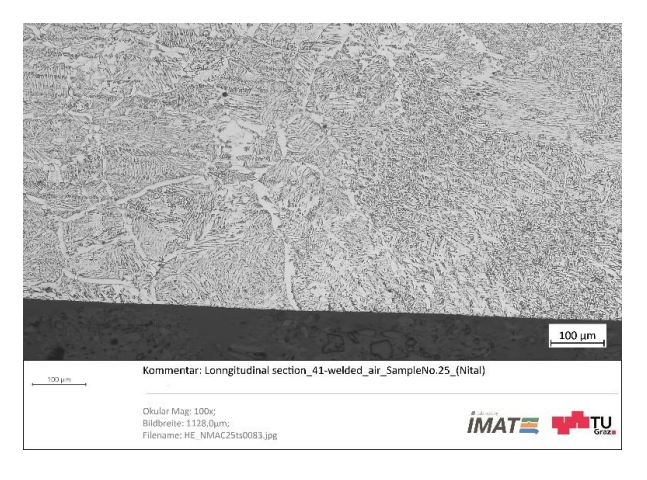


Figure 1. LOM microstructures in longitudinal sections / RSt normalized rolled (top left), CSt normalized rolled and tempered (top right) and the SAW weld of RSt (RStw).

The Vickers hardness measurements on a longitudinal section of a tested RSt tensile sample (RStw) revealed slightly elevated hardness levels of 250 HV1 in the welded area, compared to 230 HV1 in the RSt base material, thus representing an even-matched welding -s. Figure 2.

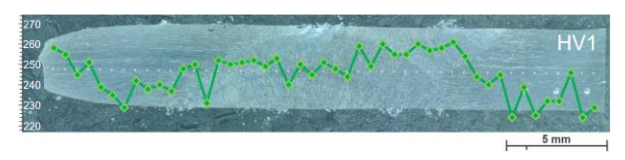


Figure 2. Hardness HV1 on a longitudinal section of a RStw tensile specimen - containing the evenmatched SAW welding.

The number of non-metallic inclusions (NMIs) larger than 6µm² and based on the standard EN 10247, in the RSt is about three times higher than in the CSt. This means, 60-100 vs. 20-30 NMIs per mm². Generally, the same types of inclusions were found in both steels, i.e. CaS, AlMgO and AlO - s. Figure 3. To note that in the CSt additionally MnSwere detected. inclusions Furthermore, incompletely molten metallic inclusions (MI) of NbTi-type (micro-alloying elements) were detected in the RSt and in the CSt, too. It cannot be ruled out that further inclusions may be present, which would require more detailed and extensive analyses.

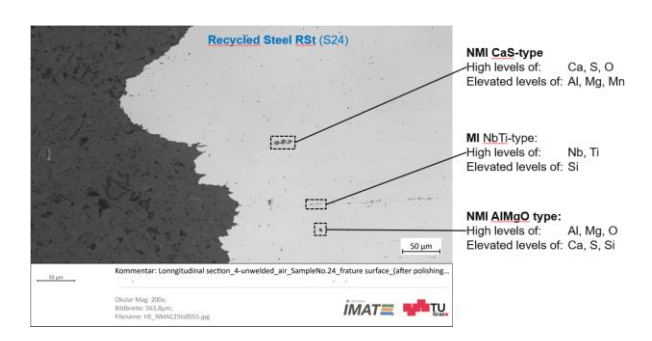


Figure 3. Types of selected NMIs in RSt in a tested tensile sample, close to the fracture (longitudinal section).

Hydrogen uptake without mechanical loading and electrochemical polarization

To assess the potential H-uptake of the investigated steels, individual specimens were subjected to charging, as described in the experimental section. The corresponding results indicate a significantly higher H-uptake of the CSt-sample after 24 hours of exposure, compared to the RSt. The latter reaches the H-saturation already after approx. 12 hours and shows a max. H-content of 0.34 wppm. In contrast the CSt has faster H-uptake and reach

a value of 0.67 wppm after 24 hours - presented in Figure, left.

The polarization tests show distinct differences as well. This means, the RSt has a higher Open Circuit Potential (OCP) of -0.67 V and is therefore more noble than the CSt exhibiting an OCP of -0.70 V vs. Ag/AgCl reference electrode. The corrosion rate evaluation using the Tafel method result in 1.8 μ m/year for the RSt vs. 4.8 μ m/year for the CSt. The cathodic branch of the RSt is larger and reach a sharp increase of H₂-formation at approx. -0.95 vs. -0.85V for the CSt - s. Figure 4, right.

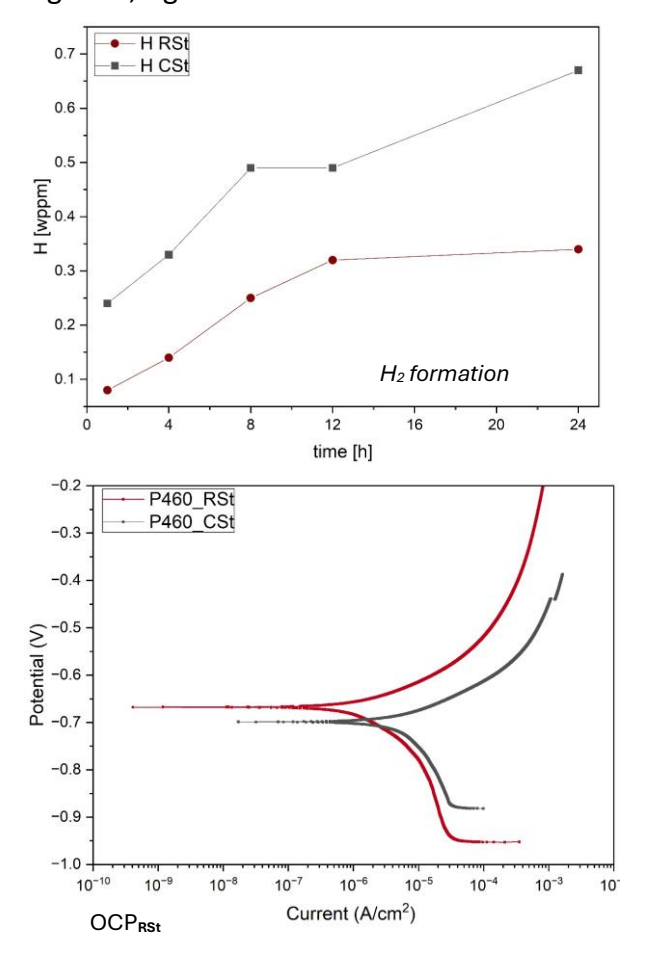


Figure 4. H-uptake in electrochemical charging (left) and polarisation curve (right) in 3.5% NaCl and 1g/L Thiourea solution vs Ag/AgCl reference electrode.

REFERENCES

[1] F. Umbach: The European Green Deal faces huge challenges; Energy Transition, February

- 10; 2020. https://www.gisreportsonline.com/r/europe an-green-deal/
- [2] L. Yang et al.: Life cycle carbon footprint of electric arc furnace steelmaking processes under different smelting modes in China; Sustainable Materials and Technologies; Volume 35, April 2023. https://doi.org/10.1016/j.susmat.2022.e005
- [3] Vallourec Expands its Range of Qualified Materials for Hydrogen Service, 02/27/2023; hydrogen-service
- [4] Sandvik to acquire the tube engineering solutions company Gerling GmbH, 2021 https://www.home.sandvik/en/news-and-media/news/2021/11/sandvik-to-acquire-the-tube-engineering-solutions-company-gerling-gmbh/
- [5] F. Passaro: A Green Future for Steel, Climate Bonds Initiative 2022; <u>www.climatebonds.net</u>
- [6] M. Elboujdaini & R. W. Revie: Metallurgical factors in stress corrosion cracking (SCC) and hydrogen-induced cracking (HIC), J Solid State Electrochem 13:1091–1099 (2009); DOI 10.1007/s10008-009-0799-0
- [7] Z. Szklarska-śmialowska, E. Lunarska: The effect of sulfide inclusions on the susceptibility of

- steels to pitting, stress corrosion cracking and hydrogen embrittlement; Materials and Corrosion, Volume 32, Issue 11, 478-485 (1981);
- https://doi.org/10.1002/maco.19810321103
- [8] N. Shikomba et al.: Resistance of welded lowalloyed pressure vessel and pipeline steels in gaseous hydrogen; Welding in the World, May 2025. https://doi.org/10.1007/s40194-025-02074-7
- [9] A. Turnbull ed.: Proceedings of Conference *Hydrogen Transport and Cracking in Metals*, 1995; ISBN 0-901716-67-7; pp. 4, 130.
- [10] G.T. Park, S.U. Koh, H.G. Jung, K.Y. Kim, Effect of microstructure on the hydrogen trapping efficiency and hydrogen induced cracking of linepipe steel, Corros. Sci. 50 (2008) 1865– 1871,

https://doi.org/10.1016/j.corsci.2008.03.007

- [11] D. Brooksbank and K. W. Andrews: Production and application of clean steels, J. Iron Steel Inst., 210 (1972), 246.
- [12] A. Hamed et al.: Assessing the hydrogen embrittlement susceptibility of an existing L360NB natural gas pipeline steel for 100 % hydrogen transport; Corrosion Science 244 (2025) 112648. https://doi.org/10.1016/j.corsci.2024.11264